

Mass-independent fractionation of mercury isotopes in Arctic snow driven by sunlight

Laura S. Sherman^{1*}, Joel D. Blum¹, Kelsey P. Johnson¹, Gerald J. Keeler², James A. Barres² and Thomas A. Douglas³

After polar sunrise in the Arctic, sunlight-induced reactions convert gaseous elemental mercury into compounds that are rapidly deposited to the snowpack. These atmospheric mercury depletion events occur repeatedly until snowmelt^{1,2}. Following deposition, the mercury can be reduced by sunlight-induced reactions and emitted as a gas³⁻⁶, or can be retained in the snowpack^{7,8}, where it may affect Arctic ecosystems following snowmelt. However, the proportion of mercury that remains in the snowpack is uncertain. Here, we measured the mercury isotopic composition of snow samples collected during an atmospheric mercury depletion event in Barrow, Alaska. We report large negative mass-independent fractionation of mercury isotopes in the Arctic snow. Results from a flux chamber experiment suggest that mass-independent fractionation is coupled to the re-emission of elemental mercury to the atmosphere, and is triggered by sunlight-induced reactions. On the basis of the above, we estimate that photochemical reactions triggered the release of a significant portion of the mercury deposited during this atmospheric mercury depletion event.

As a result of active redox chemistry, occurrence in several physical states and seven stable isotopes (196, 198, 199, 200, 201, 202 and 204 AMU), mercury (Hg) isotopes are fractionated during a wide range of reactions. Mass-dependent fractionation (MDF) of Hg can occur as a result of processes such as volatilization from aqueous solutions^{9,10} and microbial reduction¹¹. MDF is described using delta notation according to equation (1), where $(^{xxx}\text{Hg}/^{198}\text{Hg})_{\text{NIST SRM 3133}}$ is the average Hg isotope ratio of bracketing standards¹².

$$\delta^{xxx}\text{Hg}(\text{‰}) = \left[\frac{(^{xxx}\text{Hg}/^{198}\text{Hg})_{\text{unknown}}}{(^{xxx}\text{Hg}/^{198}\text{Hg})_{\text{NIST SRM 3133}}} - 1 \right] \times 1,000 \quad (1)$$

Recent data indicate that Hg isotopes can also undergo mass-independent fractionation (MIF) in which the even- and odd-mass-number isotopes fractionate from each other¹³⁻¹⁷. MIF of Hg isotopes has been observed in a variety of natural samples including sediments, hydrothermal waters and fish tissue^{10,13,16,17}. MIF is described using capital delta notation (for example, $\Delta^{199}\text{Hg}$) as the difference between the measured $\delta^{xxx}\text{Hg}$ value and that predicted on the basis of kinetic MDF (ref. 12).

Although the processes that cause MIF are not fully understood, MIF of Hg isotopes is believed to occur during both reactions at equilibrium (for example, as a result of the nuclear volume

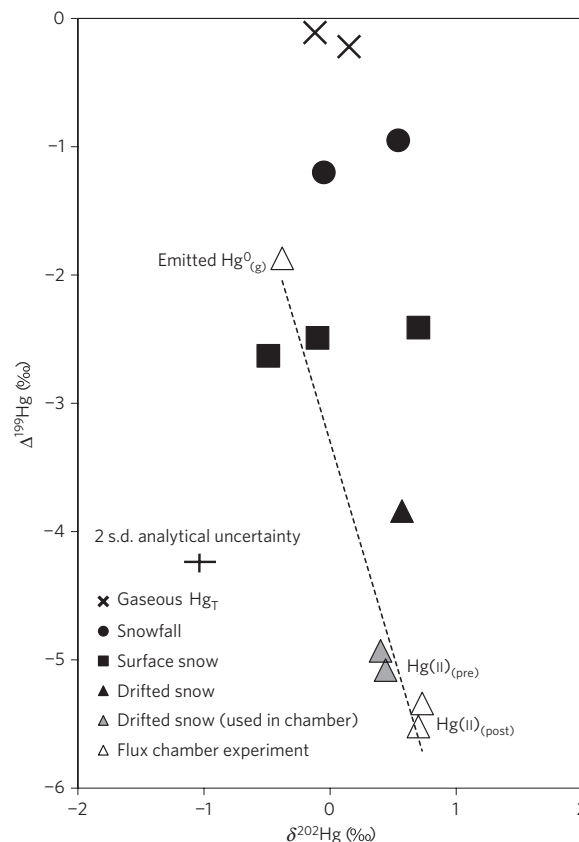


Figure 1 | Mass-dependent and mass-independent mercury isotope compositions of snow samples, chamber experiment samples and gaseous samples. Snowfall, surface and drifted snow samples are represented by filled symbols. Drifted snow samples used in the chamber are represented by grey triangles ($\text{Hg}(\text{II})_{(\text{pre})}$). Samples of snow post-experiment ($\text{Hg}(\text{II})_{(\text{post})}$) and $\text{Hg}^0_{(\text{g})}$ released during the chamber experiment ($\text{Emitted Hg}^0_{(\text{g})}$) are represented by open triangles. Gaseous Hg_T samples are represented by crosses. A linear regression based on the chamber experiment ($y = -3.30x - 3.30$; $R^2 = 0.96$) is shown as a dashed line. Representative 2 s.d. analytical uncertainty based on replicate analyses of process standards is shown.

effect)^{18,19} and kinetically driven processes (for example, as a result of the magnetic isotope effect)²⁰. The magnetic isotope effect occurs during reactions involving long-lived radical pairs

¹Department of Geological Sciences, University of Michigan, 1100 North University Avenue, Ann Arbor, Michigan 48109, USA, ²University of Michigan Air Quality Laboratory, Ann Arbor, Michigan 48109, USA, ³Cold Regions Research and Engineering Laboratory, Fort Wainwright, Alaska 99703, USA.

*e-mail: lsaylor@umich.edu.

Table 1 | Mercury isotopic compositions of standards, snow samples and chamber experiment samples.

Sample type	Hg concentration (ng l ⁻¹)	n	$\delta^{202}\text{Hg}$ (‰)	2 σ (‰)	$\delta^{201}\text{Hg}$ (‰)	2 σ (‰)	$\delta^{200}\text{Hg}$ (‰)	2 σ (‰)	$\delta^{199}\text{Hg}$ (‰)	2 σ (‰)	$\Delta^{201}\text{Hg}$ (‰)	2 σ (‰)	$\Delta^{200}\text{Hg}$ (‰)	2 σ (‰)	$\Delta^{199}\text{Hg}$ (‰)	2 σ (‰)
UM-Almadén std		151	-0.53	0.16	-0.44	0.13	-0.26	0.08	-0.15	0.08	-0.04	0.08	0.01	0.03	-0.02	0.06
NIST SRM 3133 (snow process std)		11	-0.16	0.17	-0.14	0.19	-0.09	0.11	-0.07	0.12	-0.02	0.07	-0.01	0.03	-0.03	0.09
NIST SRM 3133 (Hg _T process std)		5	-0.01	0.07	-0.03	0.08	-0.04	0.06	-0.02	0.05	-0.02	0.03	-0.03	0.05	-0.02	0.05
Gaseous Hg _T		2	-0.12	0.28	-0.13	0.32	-0.17	0.34	-0.14	0.12	-0.04	0.10	-0.11	0.20	-0.11	0.04
Gaseous Hg _T		2	0.15	0.16	0.12	0.32	0.06	0.16	-0.18	0.12	0.01	0.20	-0.01	0.08	-0.22	0.08
Snowfall	360	1	0.54		-0.38		0.19		-0.81		-0.79		-0.08		-0.95	
Snowfall	416	1	-0.05		-1.23		-0.02		-1.21		-1.19		0.00		-1.20	
Surface snow	199	1	0.70		-1.71		0.24		-2.23		-2.24		-0.12		-2.41	
Surface snow	81.2	1	-0.10		-2.45		-0.04		-2.52		-2.38		0.01		-2.49	
Surface snow	85.1	1	-0.49		-2.77		-0.26		-2.76		-2.40		-0.01		-2.63	
Drifted snow	94.5	1	0.57		-3.33		0.22		-3.70		-3.75		-0.06		-3.84	
Drifted snow	109	1	0.40		-4.32		0.12		-4.83		-4.62		-0.08		-4.93	
Drifted snow	109	1	0.44		-4.32		0.16		-4.97		-4.65		-0.06		-5.08	
Chamber expt: Hg(II) _(pre)	109	1	0.40		-4.32		0.12		-4.83		-4.62		-0.08		-4.93	
Chamber expt: Hg(II) _(pre)	109	1	0.44		-4.32		0.16		-4.97		-4.65		-0.06		-5.08	
Chamber expt: Hg(II) _(post)	96.4	1	0.73		-4.44		0.21		-5.16		-4.99		-0.16		-5.34	
Chamber expt: Hg(II) _(post)	96.4	1	0.70		-4.61		0.35		-5.34		-5.14		0.00		-5.52	
Chamber expt: Emitted Hg ⁰ _(g)		1	-0.38		-2.08		-0.24		-1.97		-1.80		-0.05		-1.87	

Average values presented for the UM-Almadén standard are based on measurements made from September 2007 to February 2009. Reported 2 σ uncertainties for the UM-Almadén standard and NIST SRM 3133 process standards are 2 s.d. of multiple measurements. Reported 2 σ uncertainties for gaseous Hg_T samples are 2 s.e. of the mean of replicate analyses. None of the snow samples contained enough Hg for Hg isotope ratios to be analysed more than once.

as a result of the influence of hyperfine coupling between unpaired nuclear spins and electronic spins on the rate of triplet to singlet spin conversion^{13,20}. Because only odd-mass-number isotopes of Hg have unpaired nuclear spins, even- and odd-mass-number isotopes can react at different rates. Bergquist and Blum¹³ demonstrated that photochemical reduction of Hg²⁺ and degradation of methylmercury from aqueous solutions containing dissolved organic carbon can cause the preferential reduction and evasion of the even-mass-number isotopes of Hg. As a result, increasingly positive $\Delta^{199}\text{Hg}$ values (up to 2.1‰ ± 0.05‰, 2 s.d.) were observed in aqueous solutions following reduction and evasion. A similar degree of positive MIF was measured in fish tissues and it was suggested that the MIF signature was passed through the aquatic food web during bioaccumulation¹³.

During polar atmospheric mercury depletion events (AMDEs), photochemically initiated reactions involving halogen and halogen oxide radicals oxidize Hg⁰_(g) in the lower atmospheric boundary layer to compounds that are rapidly deposited to the snowpack^{1,21–23}. As a result, atmospheric Hg⁰_(g) concentrations decrease significantly (to <0.5 ng m⁻³) and surface snow inorganic Hg concentrations increase (up to >250 pg m⁻³; refs 1, 21). Previous studies of Hg deposition and measurements of vertical Hg⁰_(g) profiles during AMDEs indicate that nearly total depletion of Hg occurs in the atmospheric boundary layer from the snow surface up to ~200–1,000 m elevation^{21,23,24}. Nearly complete deposition should preserve the gaseous Hg isotope composition in deposited Hg even if fractionation occurs during oxidation.

On the basis of measurements of Hg sources to the atmosphere, we expected that atmospheric Hg would not show significant MIF

(refs 10, 14). To test this we collected total gaseous Hg (Hg_T, which is predominantly Hg⁰_(g); ref. 25) near Barrow, Alaska in June 2008 by pumping filtered ambient air through gold traps. Although we did not collect gaseous samples at the same time as snow sample collection (March 2006), these atmospheric samples give us an indication of the gaseous Hg_T isotope composition in the spring near Barrow, Alaska. As expected, the Hg_T samples show very little MIF ($\Delta^{199}\text{Hg} = -0.11\text{‰}$ to $-0.22\text{‰} \pm 0.08\text{‰}$, 2 s.e.; Fig. 1 and Table 1). If removal of Hg from the boundary layer was incomplete and Hg fractionation occurs during oxidation, we cannot eliminate the possibility that the isotopic composition of deposited Hg could be different from that of Hg_T. Isotopic measurements of atmospherically deposited Hg in Spanish moss and tree lichens suggest that Hg deposited in other regions may show some negative MIF ($\Delta^{199}\text{Hg} = -0.03$ to $-1\text{‰} \pm <0.16\text{‰}$, 2 s.d.; refs 15, 26). On the basis of these data, we allow for the possibility that AMDE-deposited Hg may initially show small negative MIF ($\Delta^{199}\text{Hg} = 0$ to -1‰).

After deposition, Hg can be photochemically reduced and subsequently re-oxidized within the snow^{4,27} or released to the atmosphere as Hg⁰_(g) (refs 3–6). To investigate Hg fractionation during photochemical reduction and emission of Hg⁰_(g), we collected snowfall, surface snow and drifted snow samples during a nine-day AMDE near Barrow, Alaska in March 2006. All samples were collected using Hg-clean methods; sample collection procedures have been previously published²¹. Briefly, to avoid incorporation of saltating snow grains, snowfall was collected in trays elevated 1.5 m above the ground²¹. Newly fallen precipitation in these trays was sampled every 24 h. Surface snow was collected

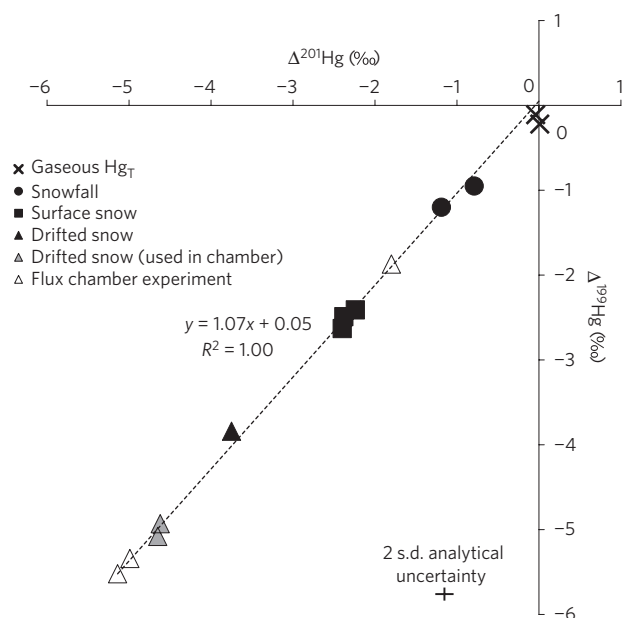


Figure 2 | Mass-independent mercury isotope compositions of snow samples and chamber experiment samples. Snowfall, surface and drifted snow samples are represented by filled symbols. Drifted snow samples used to fill the chamber are represented by grey triangles; samples of the snow in the chamber after the experiment and the $\text{Hg}^0_{(g)}$ released during the experiment are represented by open triangles. A linear regression based on all of the data is shown as a dashed line. Representative 2 s.d. analytical uncertainty based on replicate analyses of process standards is shown.

from the upper 1 cm of the snowpack and represents recently deposited snow that was exposed to sunlight for at least several days. Drifted snow was collected downwind of a wooden snow fence from the upper 2 cm of the snowpack. These samples primarily represent a mixture of snow crystals that were transported across the tundra by saltation (for an unknown distance and time period). Snowfall samples contained the highest observed inorganic Hg concentrations ($>350 \text{ ng l}^{-1}$) and concentrations were lower ($\sim 100 \text{ ng l}^{-1}$) in drifted snow samples (Table 1).

After pre-concentration, the Hg isotopic compositions of these samples were measured using cold-vapour multi-collector inductively coupled plasma mass spectrometry^{12,13} (Table 1 and Fig. 1). The amount of negative MIF increased from snowfall ($\Delta^{199}\text{Hg} = -0.95\text{‰}$ to $-1.20\text{‰} \pm 0.09\text{‰}$, 2 s.d.) to surface snow ($\Delta^{199}\text{Hg} = -2.41\text{‰}$ to $-2.63\text{‰} \pm 0.09\text{‰}$, 2 s.d.) to drifted snow ($\Delta^{199}\text{Hg} = -3.84\text{‰}$ to $-5.08\text{‰} \pm 0.09\text{‰}$, 2 s.d.). This degree of negative MIF is an order of magnitude greater than previously observed in natural samples of any type^{14–16,28}.

These data indicate that with exposure to sunlight, Hg is lost from surface snow²¹ and undergoes MIF, wherein the odd-mass-number isotopes of Hg are preferentially reduced and emitted. To further investigate the fractionation of Hg isotopes during photochemical reduction from the snowpack, we analysed the isotopic compositions of the products of a controlled flux chamber experiment. The rates of photochemical reduction for this and similar experiments were published previously²¹. On 27 March 2006, a 40 l polypropylene flux chamber with a transparent Teflon window was filled with snow from the drift site to a depth of 11.5 cm. Before starting the experiment, duplicate snow samples were taken from the chamber. Over a 10.5 h period, sunlight entered the chamber through the Teflon window and ambient air was pulled into the chamber through a Teflon inlet tube. Photochemically reduced Hg was simultaneously sampled into a Tekran 2537A gaseous Hg analyser and through an in-line gold trap

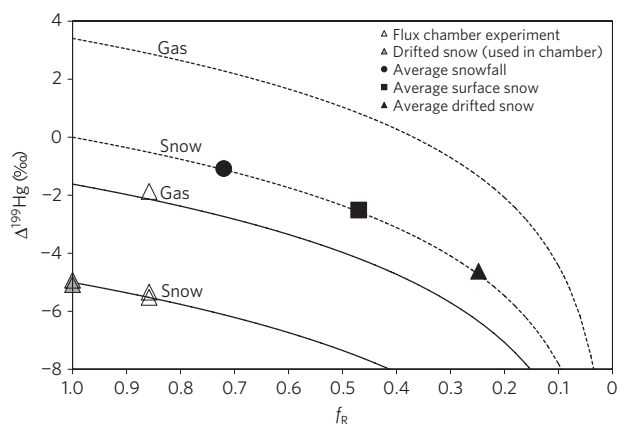


Figure 3 | Rayleigh fractionation models showing mercury isotope changes in snow and emitted gas. Flux chamber experiment samples are shown as open and grey triangles and average Hg isotopic compositions of natural snow samples are shown as filled black symbols. Models based on the chamber experiment are represented with solid lines and models of natural snow samples are represented with dashed lines. The depicted model of natural snow samples assumes that AMDE-deposited Hg does not originally show MIF (that is, $\Delta^{199}\text{Hg} \approx 0\text{‰}$).

at a combined rate of 2.5 l min^{-1} . After the experiment, duplicate samples were taken of the chamber snow (0–6 cm depth). The isotopic composition of volatilized $\text{Hg}^0_{(g)}$ collected on the gold trap was also analysed.

Photochemical reduction of Hg from the snow surface in the chamber caused both emission of $\text{Hg}^0_{(g)}$ ($\sim 6\%$ of total Hg in the snow²¹) and significant fractionation of Hg isotopes (Fig. 1 and Table 1). The measured isotopic compositions of the duplicate surface snow samples taken before the experiment were the same within measurement error ($\delta^{202}\text{Hg} = 0.40\text{‰}$ and $0.44\text{‰} \pm 0.17\text{‰}$, 2 s.d.; $\Delta^{199}\text{Hg} = -4.93\text{‰}$ and $-5.08\text{‰} \pm 0.09\text{‰}$, 2 s.d.). During the experiment, the light isotopes of Hg were preferentially lost from the snow surface (final $\delta^{202}\text{Hg} = 0.73\text{‰}$ and $0.70\text{‰} \pm 0.17\text{‰}$, 2 s.d.) and collected onto the gold trap ($\delta^{202}\text{Hg} = -0.38\text{‰} \pm 0.16\text{‰}$, 2 s.d.). Similar MDF caused by the preferential loss of light Hg isotopes has been observed during photochemical reduction of Hg from aqueous solutions^{9,10,13}. In addition to MDF, MIF was observed as a result of the preferential loss of the odd-mass-number isotopes of Hg. $\Delta^{199}\text{Hg}$ became more negative in the remaining surface snow ($\Delta^{199}\text{Hg} = -5.34\text{‰}$ and $-5.52 \pm 0.09\text{‰}$, 2 s.d.) and $\Delta^{199}\text{Hg}$ of the emitted $\text{Hg}^0_{(g)}$ was less negative than that of the original snow ($\Delta^{199}\text{Hg} = -1.87\text{‰} \pm 0.09\text{‰}$, 2 s.d.).

We suggest that MIF observed in the chamber experiment and in the natural snow samples may be caused by photochemically driven radical-pair reactions. The ratio of $\Delta^{199}\text{Hg}$ to $\Delta^{201}\text{Hg}$ for all flux chamber experiment samples and natural snow samples was $1.07 \pm 0.04\text{‰}$, 1 s.d. (Fig. 2). This value is much lower than predicted to result from nuclear volume effects (~ 2.47 ; refs 15, 18, 28). Instead, we suggest that MIF in these samples is the result of a kinetic photochemical process involving Hg–halogen radical-pair intermediates in which compounds containing odd-mass-number isotopes of Hg recombine with halogen radicals at a different rate from those containing even-mass-number isotopes. This process is similar to that observed during photochemical reduction of Hg^{2+} associated with dissolved organic matter in aquatic systems for which the measured ratio of $\Delta^{199}\text{Hg}$ to $\Delta^{201}\text{Hg}$ is $1.00 \pm 0.02\text{‰}$, 1 s.d. (ref. 13). The MIF in snow samples is, however, different because the odd-mass-number isotopes of Hg are preferentially reduced and emitted rather than retained in the oxidized form. Although we are unable to determine the specific reaction mechanisms causing the observed MIF, we suggest that

multi-step heterogeneous redox reactions are involved, probably focused in the quasi-liquid layer on the surfaces of snow crystals²⁹.

Photochemical reduction observed during the chamber experiment can be modelled using a Rayleigh-type fractionation model¹³ in which the Hg retained in the snow and the Hg emitted as Hg⁰_(g) form complementary reservoirs (Fig. 3). Although we cannot eliminate the possibility that back-reactions may affect the results of this simplistic model, we suggest that this model can provide useful insight into this complex system. To calculate a kinetic fractionation factor for this process it is necessary to know the fraction of Hg lost from the chamber snow. Previous experiments determined an e-folding depth for ultraviolet radiation in uniform Arctic coastal snow of 5–6 cm (ref. 30). On the basis of this we calculate a kinetic fractionation factor ($\Delta^{199}\alpha_{\text{snow-air}}$) of between 0.99660 and 0.99665. If the e-folding depth was greater and ultraviolet radiation penetrated to the bottom of the chamber, the calculated fractionation factor would increase only slightly to 0.99676. Assuming that AMDE-deposited Hg shows only small negative MIF ($\Delta^{199}\text{Hg} = 0$ to -1%), the Rayleigh fractionation model can be used to determine the relative amount of Hg loss that has occurred (Fig. 3). We estimate that photochemical reduction caused a loss of ~5–30% of the Hg originally in snowfall samples, ~35–50% of the Hg originally in surface snow samples and ~65–75% of the Hg in drifted snow samples.

This study demonstrates that Hg can undergo significant MIF during photochemically driven reactions in snow. Future experiments are needed to fully understand the reaction pathways involved, to explore the isotopic composition of Hg in snow during non-AMDE periods and to expand these results to other Arctic locations. We suggest that the negative MIF signature measured in AMDE-deposited Hg can be used to approximate the amount of AMDE-deposited Hg lost from the snowpack. If the remaining AMDE-deposited Hg subsequently enters Arctic ecosystems, its isotopic composition should be retained through methylation and bioaccumulation processes and would be identifiable in higher organisms.

Methods

Collection of snow samples near Barrow, Alaska (71.32° N, 156.5° W) and details of the flux chamber experiments have been described previously²¹. Snow samples and procedural standards (NIST SRM 3133 in 1% BrCl) were processed according to the following methods. BrCl (1% (v/v)) was added to the frozen samples and the snow was allowed to melt in a clean room. Inorganic Hg concentrations in the liquid snow samples were determined using atomic adsorption spectroscopy (Nippon Instruments, MA 2000) according to previously described methods²¹. For these analyses, the detection limit was 1.0 ng l⁻¹ (3 s.d. of blank analyses) and analytical uncertainty was $\pm 2.5\%$, 1 s.d.

Before isotopic analyses it was necessary to concentrate each sample into an 8 g solution with a Hg concentration of at least 2 ng g⁻¹. Hg in the samples was reduced to Hg⁰_(g) by means of simultaneous introduction of the sample and a reagent mixture (equal parts 10% SnCl₂ and 25% H₂SO₄ plus 1% by volume of 30% NH₂OH) at a rate of 0.8 ml min⁻¹ each onto a frosted-tip gas-liquid separator. A counter-flow of Ar_(g) (0.9 l min⁻¹) bubbled the resulting Hg⁰_(g) into 25 g of an acidic 2% KMnO₄ solution (Alfa Aesar, low Hg, (w/w)). Each 25 g solution was further concentrated by means of reduction in 5 ml aliquots with 20 μ l 30% NH₂OH, 250 μ l 20% SnCl₂ and 250 μ l 50% H₂SO₄. The resulting Hg⁰_(g) in these aliquots was bubbled into 8 g of 2% KMnO₄ solution using an automatic sample changer (Nippon Instruments, SC-3).

Two total gaseous Hg (Hg_T) samples were collected as part of this study (from 14 June 2008 to 18 June 2008 and from 18 June 2008 to 21 June 2008). Ambient air was pumped through 8–15 cm glass tubes containing gold beads ('gold traps') that were mounted on a polyvinyl chloride manifold and maintained at 55–65 °C to prevent condensation. Quartz-fibre filter packs were attached to the intake end of each gold trap and the flow through each gold trap was maintained at 1.8 l min⁻¹. Hg_T samples collected on gold traps and procedural standards (NIST SRM 3133 amalgamated to gold beads) were processed according to the following methods. Using a programmable heating coil, Hg was thermally desorbed from the gold beads (heat from 20 to 100 °C over 10 min; 100–300 °C over 90 min; 300–500 °C over 40 min; 500 °C for 10 min; cool). The released Hg⁰_(g) was bubbled into 25 g of 2% KMnO₄ solution with Ar_(g) at a rate of 50 ml min⁻¹. Each 25 g solution was further concentrated into 8 g using an automatic sample changer as described above.

The Hg isotope compositions of samples and procedural standards were measured according to previously published methods by means of continuous-flow cold-vapour generation multi-collector inductively coupled plasma mass spectrometry^{12,13}. Analytical uncertainties in these measurements are reported as the largest of the 2 s.d. of the long-term reproducibility of the in-house UM-Almadén standard, 2 s.d. of the reproducibility of procedural standards or 2 s.e. reproducibility of replicate sample analyses¹³. All samples reported in this study had Hg recoveries greater than 70% and procedural standards with similar Hg recoveries were not isotopically fractionated. We suggest, therefore, that all of the isotopic compositions reported in this manuscript are accurate within the reported analytical uncertainty.

MIF is described using capital delta notation according to equations (2)–(4). MIF is considered significant if it is greater than 2 s.d. of that measured in the bracketing standards (NIST SRM 3133).

$$\Delta^{199}\text{Hg} = \delta^{199}\text{Hg} - (\delta^{202}\text{Hg} \times 0.252) \quad (2)$$

$$\Delta^{200}\text{Hg} = \delta^{200}\text{Hg} - (\delta^{202}\text{Hg} \times 0.502) \quad (3)$$

$$\Delta^{201}\text{Hg} = \delta^{201}\text{Hg} - (\delta^{202}\text{Hg} \times 0.752) \quad (4)$$

Received 21 September 2009; accepted 23 December 2009; published online 7 February 2010

References

- Lindberg, S. E. *et al.* Dynamic oxidation of gaseous mercury in the troposphere at polar sunrise. *Environ. Sci. Technol.* **36**, 1245–1256 (2002).
- Steffen, A., Schroeder, W., Macdonald, R., Poissant, L. & Konoplev, A. Mercury in the Arctic atmosphere: An analysis of eight years of measurements on GEM at Alert (Canada) and a comparison with observations at Amderma (Russia) and Kuujuarapik (Canada). *Sci. Total Environ.* **342**, 185–198 (2005).
- Lalonde, J., Poulain, A. J. & Amyot, M. The role of mercury redox reactions in snow on snow-to-air mercury transfer. *Environ. Sci. Technol.* **36**, 174–178 (2002).
- Poulain, A. J. *et al.* Redox transformations of mercury in an Arctic snowpack at springtime. *Atmos. Environ.* **38**, 6763–6774 (2004).
- Steffen, A., Schroeder, W., Bottenheim, J., Narayan, J. & Fuentes, J. D. Atmospheric mercury concentrations: Measurements and profiles near snow and ice surfaces in the Canadian Arctic during Alert 2000. *Atmos. Environ.* **36**, 2653–2661 (2002).
- Kirk, J. L., St Louis, V. L. & Sharp, M. J. Rapid reduction and reemission of mercury deposited into snowpacks during atmospheric mercury depletion events at Churchill, Manitoba, Canada. *Environ. Sci. Technol.* **40**, 7590–7596 (2006).
- Dommergue, A., Ferrari, C. P., Gauchard, P.-A. & Boutron, C. F. The fate of mercury species in a sub-arctic snowpack during snowmelt. *Geophys. Res. Lett.* **30**, 1621–1624 (2003).
- St Louis, V. L. *et al.* Methylated mercury species in Canadian high arctic marine surface waters and snowpacks. *Environ. Sci. Technol.* **41**, 6433–6441 (2007).
- Zheng, W., Foucher, D. & Hintelmann, H. Mercury isotope fractionation during volatilization of Hg(0) from solution into the gas phase. *J. Anal. At. Spectrom.* **22**, 1097–1104 (2007).
- Sherman, L. S. *et al.* Mercury isotopic composition of hydrothermal systems in the Yellowstone Plateau volcanic field and Guaymas Basin sea-floor rift. *Earth. Planet. Sci. Lett.* **279**, 86–96 (2009).
- Kritee, K., Blum, J. D., Johnson, M. W., Bergquist, B. A. & Barkay, T. Mercury stable isotope fractionation during reduction of Hg(II) to Hg(0) by mercury resistant microorganisms. *Environ. Sci. Technol.* **41**, 1889–1895 (2007).
- Blum, J. D. & Bergquist, B. A. Reporting the variations in the natural isotopic composition of mercury. *Anal. Bioanal. Chem.* **388**, 353–359 (2007).
- Bergquist, B. A. & Blum, J. D. Mass-dependent and mass-independent fractionation of Hg isotopes by photo-reduction in aquatic systems. *Science* **318**, 417–420 (2007).
- Biswas, A., Blum, J. D., Bergquist, B. A., Keeler, G. J. & Zhouqing, X. Natural mercury isotope variation in coal deposits and organic soils. *Environ. Sci. Technol.* **42**, 8303–8309 (2008).
- Ghosh, S., Xu, Y., Humayun, M. & Odom, L. Mass-independent fractionation of mercury isotopes in the environment. *Geochem. Geophys. Geosyst.* **9**, Q03004 (2008).
- Hintelmann, H., Foucher, D., Telmer, K., Zheng, J. & Yamada, M. Hg isotope fractionation in sediment cores. *Geochim. Cosmochim. Acta* **72**, A379 (2008).
- Jackson, T. A., Whittle, D. M., Evans, M. S. & Muir, D. C. G. Evidence for mass-independent and mass-dependent fractionation of the stable isotopes of mercury by natural processes in aquatic ecosystems. *Appl. Geochem.* **23**, 547–571 (2008).
- Schauble, E. A. Role of nuclear volume in driving equilibrium stable isotope fractionation of mercury, thallium, and other very heavy elements. *Geochim. Cosmochim. Acta* **71**, 2170–2189 (2007).

19. Bigeleisen, J. Nuclear size and shape effects in chemical reactions. Isotope chemistry of the heavy elements. *J. Am. Chem. Soc.* **118**, 3676–3680 (1996).
20. Buchachenko, A. L. Magnetic isotope effect: Nuclear spin control of chemical reactions. *J. Phys. Chem.* **105**, 9995–10011 (2001).
21. Johnson, K. P., Blum, J. D., Keeler, G. J. & Douglas, T. A. Investigation of the deposition and emission of mercury in arctic snow during an atmospheric mercury depletion event. *J. Geophys. Res.* **113**, D17304 (2008).
22. Lu, J. Y., Schroeder, W. H., Barrie, L. A. & Steffen, A. Magnification of atmospheric mercury deposition to polar regions in springtime: The link to tropospheric ozone depletion chemistry. *Geophys. Res. Lett.* **28**, 3219–3222 (2001).
23. Tackett, P. J. *et al.* A study of the vertical scale of halogen chemistry in the Arctic troposphere during Polar Sunrise at Barrow, Alaska. *J. Geophys. Res.* **112**, D07306 (2007).
24. Banic, C. M. *et al.* Vertical distribution of gaseous elemental mercury in Canada. *J. Geophys. Res.* **108**, 4264–4277 (2003).
25. Douglas, T. A. *et al.* Influence of snow and ice crystal formation and accumulation on mercury deposition to the arctic. *Environ. Sci. Technol.* **42**, 1542–1551 (2008).
26. Carignan, J., Estrade, N., Sonke, J. E. & Donard, O. F. X. Odd isotope deficits in atmospheric Hg measured in lichens. *Environ. Sci. Technol.* **43**, 5660–5664 (2009).
27. Lalonde, J. D., Amyot, M., Doyon, M.-R. & Auclair, J.-C. Photo-induced Hg(II) reduction in snow from the remote and temperate experimental Lakes area (Ontario, Canada). *J. Geophys. Res.* **108**, 4200–4207 (2003).
28. Estrade, N., Carignan, J., Sonke, J. E. & Donard, O. F. X. Mercury isotope fractionation during liquid–vapour evaporation experiments. *Geochim. Cosmochim. Acta* **73**, 2693–2711 (2009).
29. Ferrari, C. P. *et al.* Snow-to-air exchanges of mercury in an Arctic seasonal snow pack in Ny-Alesund, Svalbard. *Atmos. Environ.* **39**, 7633–7645 (2005).
30. King, M. D. & Simpson, W. R. Extinction of ultraviolet radiation in Arctic snow at Alert, Canada (82° N). *J. Geophys. Res.* **106**, 12499–12507 (2001).

Acknowledgements

Financial support for this research was provided by the National Science Foundation Office of Polar Programs (Grants ARC-0435989 and ARC-0435893). L.S.S. is financially supported by a National Defense Science and Engineering Graduate Fellowship through the Department of Defense, Office of Naval Research. We are grateful to M. W. Johnson, L. Alvarez-Aviles, M. Sturm, R. Prevost, P. W. Sherman and the members of BEIGL for assistance and helpful discussions.

Author contributions

J.D.B. initiated this study along with T.A.D. and G.J.K. K.P.J., J.D.B., T.A.D., J.A.B. and G.J.K. collected the snow samples and conducted the chamber experiment. L.S.S. and K.P.J. conducted the laboratory analyses and L.S.S. wrote the manuscript. All authors contributed to discussions of results and conclusions.

Additional information

The authors declare no competing financial interests. Reprints and permissions information is available online at <http://npg.nature.com/reprintsandpermissions>. Correspondence and requests for materials should be addressed to L.S.S.